HCIS | Human-centric Computing and Information Sciences

RESEARCH (Research Manuscript) **Open Access**

Human-centric Computing and Information Sciences (2023) 13:16
DOI: https://doi.org/10.22967/HCIS.2023.13.016
Received: October 14, 2021; Accepted: November 25, 2021; Published: April 15, 2023

Role of Sensors Based on Machine Learning Health Monitoring in Athletes' Wearable Heart Rate Monitoring

Wei Ding*

Abstract

As domestic athletes and other sports become more and more popular, the health protection of athletes has gradually attracted people's attention, and the heart rate monitoring of machine learning sensors has gradually been understood by people. In order to in-depth study the current status of the role of machine learning sensors in wearable heart rate monitoring, this article uses the new and old sensor comparison method, the field survey method and the human sample test method, collects samples, analyzes the machine learning sensor, and streamlines the algorithm. And create a sensor for wearable heart rate monitoring. In studying the innovation and improvement of the comparison between the new sensor and the old one, this paper uses the shimmer node on the Tiny-OS platform to collect a total of 36 sets of heart rate data of three men and three women in different exercise states, and uses two types of algorithms to calculate the results. It shows that the calculation time of the algorithm proposed in the paper is 0.21, the traditional electrocardiogram (ECG) algorithm is 0.28, and the new algorithm has lower time complexity. Research on the accuracy of the sensor in practical application shows that the recognition rate of riding a bicycle is almost close to 1.00, which fully meets the 0.96 recognition requirement of this system. Although, the single recognition rate of standing still did not reach 0.95. However, the total average recognition rate of the nine sports is 0.971, which is already above 0.96, which proves that the average recognition rate of the monitoring system is above 96%. The system is considered to be a basic design success. It is basically realized that starting from the wearable heart rate monitoring, a machine learning sensor that can be put into large-scale application is designed.

Keywords

Machine Learning, Heart Rate Monitoring, Wearable Sensors, Remote Monitoring, Model Process

1. Introduction

Entering the 21st century, China has entered a period of rapid economic development, and the overall living standards of the society have greatly improved. However, people have more and more sports activities, which leads to higher and higher health risks for people. Because of their vigorous exercise range and amount of exercise, athletes also have various minor problems in their bodies and their health is seriously threatened. The research in this paper mainly includes walking, running, up and down stairs,

***Corresponding Author:** Wei Ding (20060116@sdufe.edu.cn)
College of Physical Education, Shandong University of Finance and Economics, Jinan, China

up and down, cycling and other sports. By tracking and monitoring these exercises, we can indirectly understand the health of the human body. There are many ways to track and monitor the daily movement of the human body, one of which is to use video surveillance based on image vision. Although this method can effectively monitor the daily movement of the human body, it has many obvious shortcomings. At present, with the development of machine learning and the gradual maturity of technology, health monitoring sensors are gradually being applied to all areas of life. This paper is to use this type of sensor to track and monitor athletes' daily sports.

Human electrocardiogram (ECG) and heart rate, and transmit the detection results to remote places in real time. The medical monitoring institution of China provides immediate monitoring of the athletes on the field to provide the athletes with maximum health and safety protection. The thesis first analyzes and studies machine learning, health monitoring sensors, various related communication technologies, and wearable sensor technologies. Secondly, it focuses on two important physical parameters in remote health monitoring: ECG signals and fall parameters, and the detection algorithms of the two types of parameters are analyzed and optimized, which improves the accuracy of the detection algorithm and reduces the computational complexity of the algorithm.

The innovations of this paper are (1) based on the theory of small radius bending loss of sensor fiber, a new method of partially cutting off the fiber cladding to eliminate the weak transmission signal when the fiber is bent in a large angle range is proposed; (2) using the sensor The monotonicity of optical fiber bending loss, a large strain sensor with a maximum strain of 60% is designed, which has good compatibility with measuring heart rate and can be used in collision monitoring between athletes; (3) developed a sensor-based sensor The fiber-optic large-strain test system realizes real-time heart rate monitoring of the strain and behavior process of test subjects under laboratory conditions, and is expected to play an important role in real-time protection of athletes. Through the above work, the effectiveness, accuracy, transmission efficiency and signal integrity of the health monitoring sensor based on machine learning in monitoring the athlete's heart rate are improved.

2. Related Work

Sports competitions are exciting, intense, and hidden dangers. In order to protect athletes, in the current situation where machine learning is so popular, is it feasible to apply it to athletes' heart rate monitoring? Some foreign scholars have already given their answers. Wang and Verma [1] derive classification decisions from analog sensor signals, and proposes a machine learning algorithm for training classifiers, which can overcome circuit imperfections in analog circuits and severe energy/area scaling. In addition, the noise model of the system was proposed and verified through experiments, providing a method for predicting and optimizing the probability of classification errors in a given application. Zhang et al. [2] use ubiquitous wearable devices to develop a wearable crowdsourcing system to monitor respiratory symptoms such as cough and fever. Preliminary results show that our algorithm achieves higher detection accuracy and fewer false positives with the lowest utilization rate of computing resources. This research may change the way we implement pandemic early warning and how we respond to public health crises in the coming years. Liao et al. [3] proposed an effective and stable HGU fault diagnosis system based on sequence data structure using one-dimensional convolutional neural network (1-D CNN) and gated recurrent unit (GRU). Based on the experimental dataset, four machine learning methods are applied to diagnose the reconstructed data. By comparing with the results of other machine learning techniques, the performance of the proposed method is verified. Goyal et al. [4] designed and developed a non-contact vibration sensor to obtain vibration data for bearing health monitoring under load and speed changes. The results show that the vibration characteristics obtained from the developed non-contact sensor (NCS) compare well with the accelerometer data obtained under the same conditions. He et al. [5] proposed a robust heart rate monitoring scheme for different quasi-periodic motions using wrist photoplethysmogram (PPG), the heart rate-related spectrum peak tracking and the spectrum peak tracking. The proposed scheme is robust to MA caused by different motions and has high accuracy.

Experiments on six common quasi-periodic exercises show that the average absolute error of heart rate estimation is 2.40 beats per minute (bpm). The proposed method is more robust than some state-of-the-art methods for different sports. Li et al. [6] introduced the use of sensors for heart rate monitoring. When the sensor with a bracket is worn on the human body, the heart rate can be accurately monitored by monitoring the laser intensity changes caused by the heartbeat. Experimental results show that the strain sensitivity of the sensor is 2.57 pm/μN , which has good adaptability and can measure the heart rate of different parts of the human body, such as the wrist, chest, and neck. Xie et al. [7] proposed an unobtrusive system for monitoring heart rate based on ballistocardiogram (BCG). The system includes a piezoelectric sensor that can be embedded in a chair or bed to convert tiny body vibrations caused by heartbeats into BCG signals, and a new algorithm for estimating heart rate from BCG. The performance of the proposed algorithm was evaluated by BCG records from 32 subjects. Achieved a mean absolute error (MAE) of 2.17 bpm and a standard deviation of absolute error (SDAE) of 2.34 bpm. The physiological signals obtained by Lin et al. [8] through heart rate and blood pressure monitoring are used to assess mental stress, which can be recommended to inform the individual's mental state. It proposes an artificial intelligence-based fuzzy assisted Petri net (AI-FAS) method for stress assessment of heart rate and blood pressure monitoring. The variance of the heart rate is measured by time and frequency analysis. Cicceri et al. [9] collected data from inertial sensors. The purpose is to design and implement a non-invasive system of wearable sensors based on the human-centered computing (HC) paradigm, and prevent primary user (PU) technology through deep learning. A dataset was established by monitoring the location of a group of patients during hospitalization. We show the results here, demonstrating the feasibility of the technology and the level of accuracy we can achieve, and comparing our model with other popular machines. Tang et a. [10] studied the characteristics of network traffic, using variance and entropy to evaluate the characteristics of TCP traffic, and analyzed the ratio of UDP traffic to TCP traffic. Therefore, a detection method combining two-step cluster analysis and UTR analysis is proposed. Through the two-step cluster analysis as one of the machine learning algorithms, the network traffic is divided into multiple clusters, and then the UTR analysis is used to determine the clusters subject to low-rate DoS attacks. These studies have provided a good reference for this article, but there are some related studies, such as the unknown source of experimental data, and the fact that the experimental variables have not been effectively controlled. As a result, the results of the experiment have not been convinced by the public.

3. Implementation Method of Research based on the Role of Machine Learning Sensors in Athletes' Heart Rate Monitoring

3.1 Machine Learning

Machine learning is a computer theory that imitates the human thinking mode. In the 1960s, machine learning emerged and included various subjects such as probability and statistics in the early days. After that, algorithms related to machine learning occupy an unshakable position in the academic world. With the continuous development and update of computer technology, the corresponding computer hardware has also been rapidly developed, and the earth-shaking changes brought about by the computing speed to our lives will also become an indispensable part of our lives. The products of machine learning are also found in all aspects of life, such as the Google search engine, Google pictures, and many systems that process visual information that we often come into contact within our lives. Machine learning drives the development of enterprises. At present, large domestic Internet companies such as Evergrande, Country Garden, Meizu, OPPO, Huawei, etc., and many small entrepreneurial companies are vying to apply machine learning knowledge to produce products suitable for people’s needs.

The supervised learning included in machine learning is a learning method in which the data samples in the input algorithm model are labeled or a training method in which the training samples in the training dataset have the correct classification results. After training the model, if the test data in the test set is

input, and the corresponding output is a continuous number, we call the model a regression analysis model; if the output value of the model is not a specific value but a classification label value of, we call classification analysis. The training process of the supervised learning model is shown in Fig. 1.

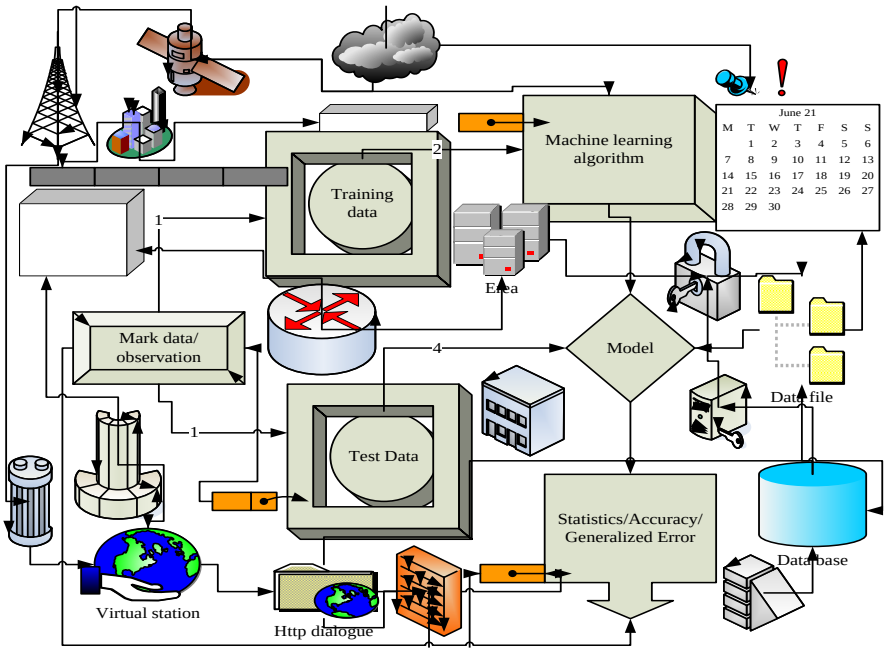

Fig. 1. Flow chart of supervised learning.

From Fig. 1, we can see that for a label-based machine learning algorithm, the first task of the algorithm is to learn the input training data, use the learned model to predict a new case, and give the output value of the case, the model use the output value given by itself and the standard value to calculate the loss value, and then backpropagate to adjust the model parameters of the supervised learning algorithm. To make the model achieve a precise classification effect, it is necessary to input more data to the model and conduct a lot of training on this basis.

3.2 Heart Rate Monitoring

The heart rate can be displayed on the ECG. The bioelectricity that changes regularly occurs during the beating of the heart. This bioelectricity will spread to the surface of the body along with body fluids and conductive tissues, which is embodied in the changes in potential amplitude, period and direction. Medical staff can use external electrodes to collect these bioelectric signals and display them as a time-varying curve through the output of medical instruments, which is an ECG. As shown in Fig. 2, a healthy standard ECG is composed of different wave groups. If the heart of the human body has any disease, it is reflected in the ECG as a distortion of the wave group shape.

As shown in Fig. 2, the standard ECG mainly contains P wave, P-R wave band, QRS wave band, S-T wave band, T and Q-T wave groups. Different bands represent the changes in ECG at different stages [11]. The ECG detection algorithm currently used mainly diagnoses characteristic waves such as P wave, QRS wave, and T wave.

P wave: As one of the three characteristic waves of the ECG, P wave reflects the electrical activation process between the left and right chambers of the heart. The healthy P-wave width should be less than 0.111 seconds, and the peak amplitude should be greater than 0.24 mV. The strict ECG detection algorithm needs to confirm the P wave in addition to the QRS signature wave [12].

QRS complex: QRS characteristic wave is the main research object of the ECG detection algorithm, which mainly reflects the electrical activation process of the left and right ventricles of the heart, and is the wave group with the largest fluctuation amplitude in the electrocardiogram. The QRS characteristic wave is composed of Q wave, R wave, and S wave. A healthy QRS waveband should be less than 0.1 seconds in width.

T wave: If P wave symbolizes the beginning of a heartbeat, then T wave means the end of this beat. As one of the characteristic waves of ECG, P wave reflects the potential changes brought about by the recovery of cardiac myocardium, with small amplitude and long duration [13].

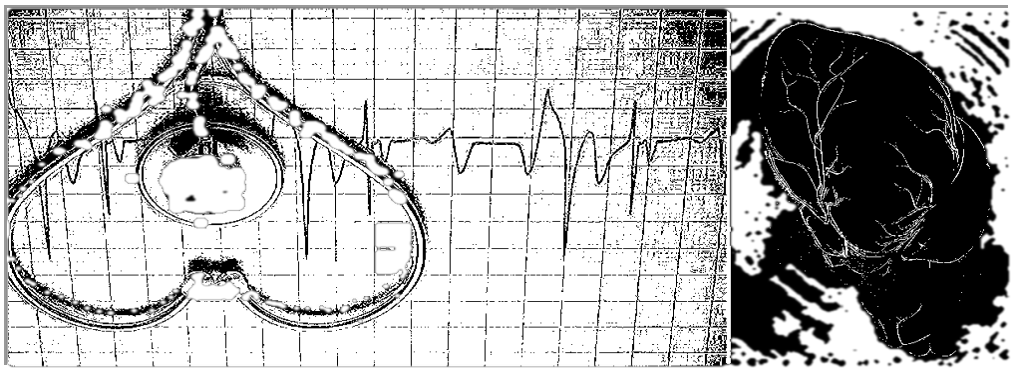

Fig. 2. ECG standard waveform. Picture reference can be seen at http://m.sohu.com/a/315890697_99902329 and http://upload.ilinyi.net/2014/1210/1418194399835.jpg.

3.3 Wearable Sensors

In the architecture of the article, wearable sensor nodes are the most important link [14]. With the improvement of wireless communication technology, the widely used sensor nodes have a lot of built-in functions, and their data collection and real-time processing capabilities are also better. For ECG, blood oxygen, blood pressure, pulse, body temperature, brain wave (electroencephalogram [EEG]), and other physical signs, nodes can effectively complete data collection and real-time analysis [15]. In addition to these characteristic parameters of the human body, environmental parameters such as humidity, light intensity, temperature, etc., around the monitored object can also be collected and transmitted through the node. Fig. 3 describes the system from the sensor to the wearable heart rate monitoring in detail (http://www.chinagongcheng.com/supply/3_33521666.html).

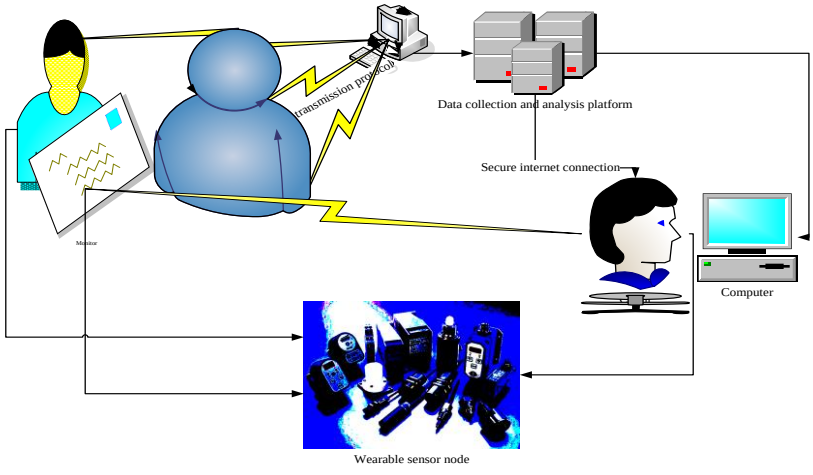

Fig. 3. Wearable sensor architecture.

As shown in Fig. 3, these wearable nodes collect various physiological characteristic parameters of the human body and complete the data integration processing work in the nodes, and then use the preset anchor nodes in the wireless communication network for information transmission, and gradually concentrate on the sink nodes, and finally transmitted to the medical monitoring terminal. After the monitoring terminal obtains the data, it first classifies and analyzes the physiological signal data, and accurately judges the health status of the monitored object, and finally saves the judgment result and data into the database for later reference [16].

3.3.1 Information matrix criteria

When the sensor tests the structure with experimental data of the modal mode, select the appropriate mode order to ensure that the modal data can be fully measured, and use the generalized coordinate *h* of the modal mode as the parameter to be identified, then the output of the sensor can be expressed as:

$$v_t = \beta_t h \sum_{exp}^{uzi\Sigma} (v_i v_l v_j) \tag{1}$$

where *t* is the number of candidate measuring points, v_t is the output information of the sensor, and β_t is the theoretical modal matrix calculated by the finite element model [17]. Generally, the structure has more degrees of freedom, and the number of sensors tested is limited. Assuming that there are only n sensors, the entire structure has *t* degrees of freedom placement positions. In order to obtain the modal information of the structure as much as possible for the limited *n* sensors. To achieve the best estimate of the target mode, we need to determine the position of the sensor on all degrees of freedom, that is, to minimize the covariance matrix of the estimation error of the parameter h to be identified to meet the best estimate [18]. Considering the influence of noise, the revised output expression is obtained through research:

$$v_t = g(h) + t = \beta_t h + t \tag{2}$$

where $g(h) = \beta_t h$ and vector *t* represent Gaussian white noise with variance β_0^2 [19]. The covariance matrix of the estimation error of the parameter h to be identified is an unbiased estimation, which can be expressed by the following formula:

$$q = k\left[(\mathrm{h}\text{-}\hat{\mathrm{h}})(h - \hat{h})^s\right] = \left[\left(\frac{\varepsilon g}{\varepsilon h}\right)^s [\beta_0^2]^{-1} \left(\frac{\varepsilon g}{\varepsilon h}\right)\right]^{-1} = h_{\beta}^{-1} \tag{3}$$

Among them, *k* represents the mathematical expectation, and $\hat{h}$ represents the estimated value of *h*. Because the test noise is static Gaussian white noise, it is a fixed value when measuring modal data [20]. Then the information matrix can be expressed as:

$$h_{\beta} = \frac{1}{\eta} \beta^s \beta \tag{4}$$

where h_{β} is the information matrix based on the mode shape, which can well reflect the characteristics of the mode shape. In order to minimize the estimation deviation of *h*, that is, to obtain the best estimate of *h*, the information matrix determinant, trace and norm can be used the maximum number, the more information content [21].

When the information matrix is used as the evaluation criterion, the ratio of the determinant of the information matrix formed after deleting the modal shape of the measuring point every time to the value of the original information matrix can be expressed as:

$$\pi = \frac{wks(h')}{wks(h_0)} * 99\%(k_p - k_a)wps \tag{5}$$

Among them, h_0 is the original information matrix, and h' is the new information matrix formed after deleting a candidate measuring point each time. The larger the π, the more information content of the measuring point, and the better the method of arranging measuring points [22].

3.3.2 Maximum singularity ratio

The maximum singular value ratio after singular value decomposition of the modal matrix can be used as an index to measure the effect of sensor placement. The singular value of the modal matrix β can be obtained by the singular decomposition theorem of the matrix. Assuming $x \in \beta_{o,n}$, let *h*=max{n,o} and class *x*=*t*, then there are unitary matrices $u \in \beta_o$ and $d \in \beta_n$, and a diagonal matrix

$$\sum h = \begin{bmatrix} \varepsilon_1 & \cdots & 0 \\ \cdots & \cdots & \cdots \\ 0 & \cdots & \varepsilon_h \end{bmatrix} * \left[(kp - ka) \sum_{exp}^{uzi\Sigma} (\hat{h} - \hat{h}) [] \right] \tag{6}$$

So that $\varepsilon 1 \geq \varepsilon 2 \geq \cdots \geq \varepsilon s > 0 = \varepsilon_{s+1} = \cdots = \varepsilon h$ and $x = u \sum d^*$

$$\sum = \begin{cases} \sum h & orn = o \\ \left[\sum h \quad 0\right] \in \beta_{o.n}, & orn > o \\ \left[\sum h \quad 0\right]^s \in \beta_{o,n}, & orn < o \end{cases} \tag{7}$$

Among them, the parameter is the positive square root of the non-zero eigenvalues of *xx** arranged in descending order. The singular value *t* of *x* is uniquely determined by the eigenvalue of *xx** [23].

The basic idea of the model reduction criterion is to divide the structural degrees of freedom into primary and secondary degrees of freedom, retain the primary degrees of freedom through model reduction, eliminate the secondary degrees of freedom, and arrange sensors on the primary degrees of freedom to measure the response of the structure. The state vector *h*, the load vector l, and the system matrices *n* and *p* are split into master and slave degrees of freedom. The degree of freedom that is not subject to external force is selected as the slave degree of freedom.

The second-order vibration differential equation of structure is:

$$nv(s) + zv(s) + gv(s) = l(s) \tag{8}$$

where n is the mass inertia matrix, z is the damping matrix, g is the stiffness matrix, and $l(s)$ is the external load. Assuming that the damping term is ignored, the motion equation of the structure is:

$$\begin{bmatrix} n_{nn} & n_{nt} \\ n_{tn} & n_{tt} \end{bmatrix} \begin{bmatrix} \cdots \\ h_n \\ \cdots \\ h_t \end{bmatrix} + \begin{bmatrix} g_{nn} & g_{nt} \\ g_{tn} & g_{tt} \end{bmatrix} \begin{bmatrix} h_n \\ h_t \end{bmatrix} = \begin{bmatrix} l_n(s) \\ 0 \end{bmatrix} \tag{9}$$

The subscript n is the master coordinate system, and t is the slave coordinate system. Ignoring the inertia term of the second equation, you can eliminate the degree of freedom, as follows:

$$\begin{bmatrix} h_n \\ h_t \end{bmatrix} = \begin{bmatrix} j \\ -g_{tt}^{-1} \quad g_{tn} \end{bmatrix} [h_n] = s_t h_n \tag{10}$$

In the formula, the matrix s_t represents the static conversion matrix between the state vector before reduction and the primary coordinate system [24]. The reduced mass matrix and stiffness matrix are:

$$n_i = s_t^s n s_t \left[\sum st^{-1}\right] exp$$
$$g_i = s_t^s g s_t \tag{11}$$

3.3.3 Effective independence method

The principle of the effective independence method is to gradually delete the degrees of freedom from all the degree of freedom measurement points. These deleted degrees of freedom should minimize the change in the determinant value of the information matrix until the number of measurement points arranged is reached. The remaining modal pairs of the measurement points The linear independence contributes the most, and the best estimation of the mode shape is obtained to realize the optimization of the sensor layout and define the sensor output response as v_t, then

$$v_t = \beta_t h = \sum_{u=1}^{o} \beta_u h_u \tag{12}$$

Among them, h is the modal coordinate, β_t is the measured $o \times o$-order modal matrix, o is the number of degrees of freedom, O is the modal order, β_u is the u-th modal mode shape, and h_u is the mode participation coefficient.

The least square solution of the modal coordinate h in formula (13) is:

$$\hat{h} = [\beta_t^s \beta_t]^{-1} \beta_t^s v_t \tag{13}$$

Considering the noise t, the response can be expressed as:

$$v_t = \beta_t h + t = \sum_{u=1}^{o} \beta_u h_u + t \tag{14}$$

Corresponding to the deviation of $\hat{h}$, assuming an unbiased effective estimate, the covariance matrix q of the estimated deviation can be expressed as:

$$q = k\left[(h - \hat{h})(h - \hat{h})^s\right] = h^{-1}$$
$$h = \frac{1}{\eta^2} \beta_t^s \beta_t = \frac{1}{\eta^2} x_0 \tag{15}$$

Among them, h is the information matrix. When x_0 takes the maximum value, h also takes the maximum value. Therefore, x_0 can be used to reflect h. After obtaining the matrix E, the measurement points are sorted in order by the size of the diagonal elements of the E matrix, and the measurement points with the smallest diagonal elements corresponding to each iteration of the calculation are excluded, and then the next iteration is carried out until the need to be retained up to the number of measuring points [25]. Through multiple iterations, the modal matrix is linearly independent as much as possible, which better reflects the characteristics of the original structure.

4. Realization Method Experiment Based on the Study of the Role of Machine Learning Sensors in Athletes' Heart Rate Monitoring

4.1 System Architecture

The heart rate monitoring sensor designed in this article is a distributed system composed of wireless sensor nodes, coordinators, and data transmission modules, as shown in Fig. 4. The cluster-based hierarchical structure has natural distributed processing capabilities. The cluster head is the distributed

processing center, which is a coordinator of the wireless sensor network in this article. Each cluster member (sensor node) transmits data to the cluster head. After data fusion, it is directly transmitted to GSM (global system for mobile communication) for data transmission. The central control center is connected to multiple coordinators through the GSM network. The coordinator and sensor nodes realize wireless information exchange through Zigbee technology. The wireless sensor node with radio frequency transceiver is responsible for the perception and processing of data and transmits it to the coordinator; The control center obtains the collected relevant information through the GSM network to realize effective control and management of the scene.

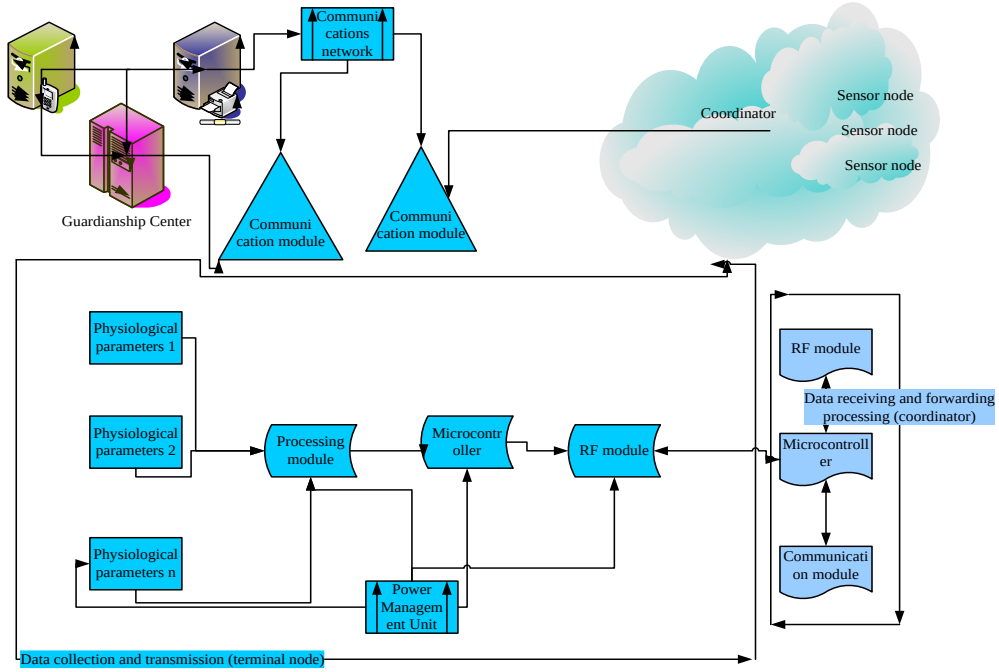

Fig. 4. The overall architecture of the remote health monitoring system.

It can be seen from Fig. 4 that the terminal node structure includes physical sign sensors, conditioning circuits, microcontroller unit (MCUs), RF modules, and power supplies. Since this node is to be worn on the user's body, its volume and weight should be as light as possible. The coordinator is responsible for receiving and preliminary analysis and processing of the data sent by several nodes, and then sending the data through the microcontroller connected to the communication module. Because the communication network (such as the GSM network) has a wide coverage and relatively complete performance, it also has a strong data error correction capability, which can ensure the reliability and real-time performance of data transmission, and can effectively reduce system costs.

4.2 Heart Rate Sensor Selection

In the exercise heart rate monitoring designed in this article, we mainly monitor the athlete's pulse, so we mainly consider the selection and application of the pulse sensor (piezoelectric sensor) in the sensor module. At present, there are a variety of sensors for collecting weak human signals, such as piezoelectric ceramic sensors, Doppler effect sensors, etc., but there are certain problems in structure and cost. At present, there is a piezoelectric sensor using a new type of polymer piezoelectric material polyvinylidene fluoride, which has a simple structure, high sensitivity, and can accurately measure weak human signals. We use its advantages to measure human pulse signals and other piezoelectric materials. In comparison,

it has the advantages of large piezoelectric coefficient, wide frequency response, easy matching of acoustic impedance, high mechanical strength, good flexibility, light weight, impact resistance, easy large-area film formation and low price. The piezoelectric strain constant of PVDF piezoelectric film is 12 times that of quartz crystal, and the piezoelectric voltage constant is the highest among all piezoelectric bodies. The PVDF is larger than the crystal from the perspective of the electromechanical damage coefficient. Their acoustic impedance rate is less than that of inorganic piezoelectric crystals. This shows that the polymer piezoelectric plastic has excellent mechanical properties and a wide frequency response range, and is an ideal sensor material. The piezoelectric film of the sensor is a kind of polymer functional sensing material, and its main characteristics are shown in Table 1.

The main performance indicators of the heart sound heart rate sensor made of PVDF materials can be summarized as shown in Table 2.

Table 1. Specific parameters of PVDF piezoelectric film

Parameter	Numerical value
Broadband	0.002–10^8 Hz
Wide dynamic range	10^{-7}–10^5 pc
Low acoustic impedance	2.6 times as much as water, easy to match
High flexibility	Good flexibility, easy to close to the human body
High sensitivity	The output signal is more than 10 times higher than piezoelectric ceramics
High dielectric strength	Can withstand strong electric field (80 V/μm)
High mechanical strength and impact resistance	10^8–$10^{9.5}$
High stability	Moisture resistance (hygroscopicity <0.03%)
Easy to process	Can be processed into specific shapes
Easy to install	Can be fixed with commercially available glue

Table 2. Main performance indicators of the heart sound pulse sensor

Index	Number
Frequency response	0.04–1.45 Hz + 2.5 dB
Sensitivity	>3.5 mV/kP
Insulation resistance	>105 mu
Output impedance	<1 wu
power supply	+4.5–14.5 uwz
Output cable	3 cores

4.3 Main Business Realized by the Sensor

4.3.1 Heart rate notification service

When athletes register for the heart rate notification service, they need to choose different notification methods, service modes and other information. After wearing the heart rate sensor and starting the heart rate notification service, the athlete will get the heart rate information sent by the host according to the customized notification mode. There are three specific notification methods. One is a manual method. The host will display a message to the host console. The content of the message is: the athlete's name, the athlete's phone number, and the athlete's heart rate per minute. Another way is SMS. The host sends the following SMS directly to the athlete: "'Athlete's name', your current heart rate is XX beats per minute." The third method is the silent method, where the host directly stores the data in the database and waits for the athletes to query. After each inspection and information is sent, all messages must be included in the database in the form of inspection results and result reports.

4.3.2 Heart rate query business

Athletes can log on to the Internet to inquire about changes in body temperature at the check frequency of their choice during a certain period of time. The host side generates reports and charts, and feeds them back to the athlete's browser.

4.3.3 Athlete management business

As a basic business module, this business completes the registration, modification, deletion and identity authentication of athletes.

5. Experimental Results based on the Design and Implementation Method of the Research on the Role of Machine Learning Sensors in Athletes' Heart Rate Monitoring

5.1 Survey Content and Sample Analysis

In order to conduct a more comprehensive experimental verification of the proposed algorithm, this paper uses the shimmer node on the Tiny-OS platform to collect a total of 36 sets of heart rate data from six different individuals (three males and three females) in the laboratory under different exercise states, and uses two The algorithms are calculated separately (among which, the calculation results of the heart rate detection algorithm based on QRS feature wave positioning are the results obtained under the premise of ensuring that all QRS feature waves are accurately located during the interception period). The calculation results are compared as shown in Fig. 5.

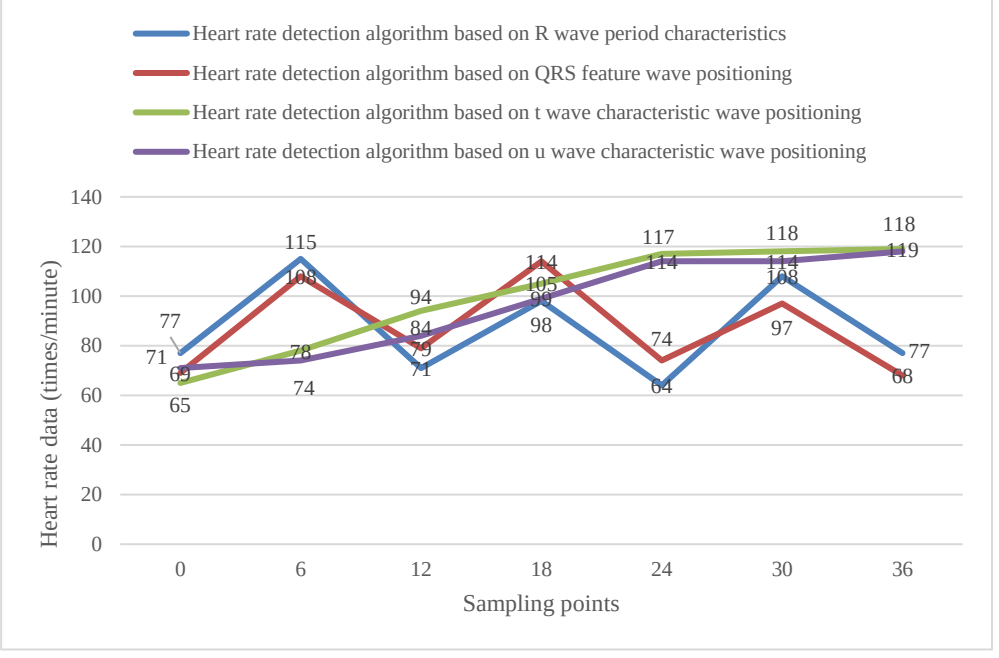

Fig. 5. Comparison of heart rate calculation results of two types of ECG detection algorithms.

It can be seen from Fig. 5 that in order to verify the superiority of the paper's algorithm in terms of time complexity, this paper uses the same computer (that is, the same hardware and the same software environment) to perform algorithmic time statistics on the above 30 sets of data. The results are as shown in Fig. 6.

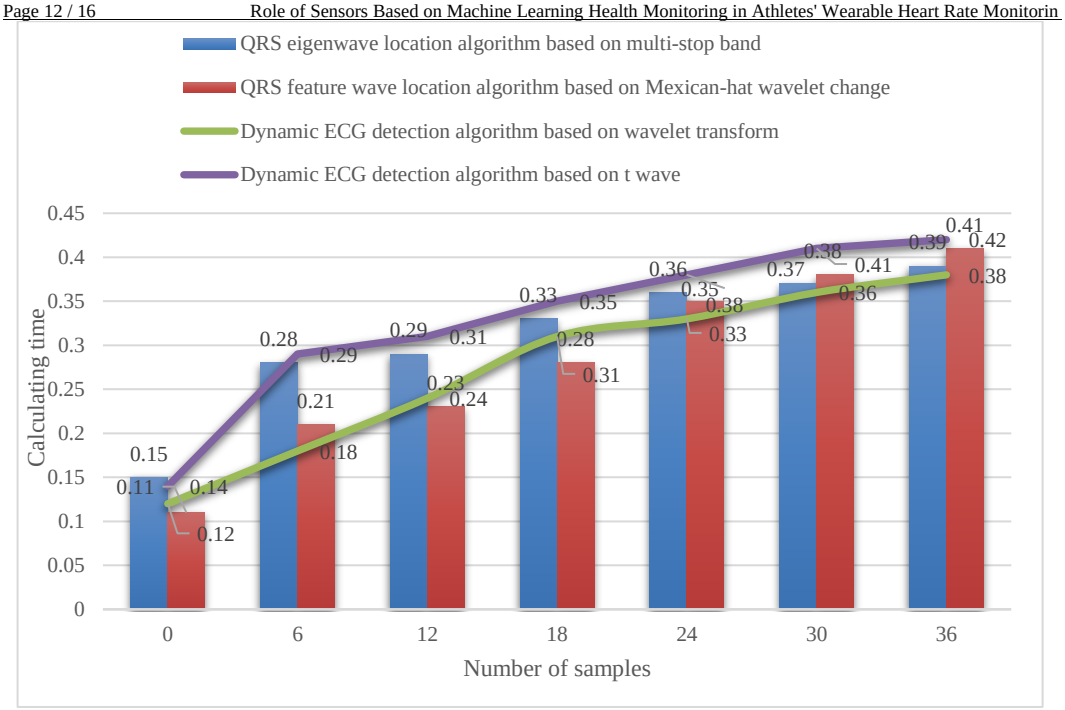

Fig. 6. Comparison of time complexity of different types of ECG detection algorithms.

From the experimental results in Fig. 6, it can be found that no matter what the state of motion of the guardian, the dynamic ECG detection algorithm based on wavelet transform and short-term autocorrelation transform proposed in the paper can basically keep the same with the traditional ECG algorithm in terms of heart rate calculation., And the time complexity is lower. Therefore, it can be proved that the ECG detection algorithm based on R wave-like periodic characteristics proposed in the paper can effectively ensure the calculation accuracy of heart rate while reducing the algorithm's denoising dependence and computational complexity, which meets the practical needs of the system.

The thesis is based on the Tiny-OS platform, using the three-axis of the node and the machine learning sensor module to collect a set of simulated fall data, with a sampling rate of 12 times per second. This set of data simulates the situation in which athletes may move out of balance and fall in four directions, respectively, in the walking state. For the collected three-axis motion data, the paper processed the data based on the characteristics of SMV, energy and inclination. The processing results are shown in Fig. 7.

It can be seen from Fig. 7 that at the moment the human body falls, the acceleration values in the X- and Y-axis directions will fluctuate, so that the characteristic values of SMV and energy will instantly increase, and the inclination value will also increase instantaneously. Combined with the judgment process based on multiple thresholds proposed in the paper, the algorithm can accurately judge the athlete's several falls during this period. In order to verify the effect of the algorithm, the paper arranged for five experimental subjects to wear shimmer machine learning sensors to collect 30 sets of falling data in different states, and compare them with the fall detection algorithm based on a single feature value SMV. The detection results are shown in Fig. 8.

It can be found from the experimental results in Fig. 8 that in a steady state, the fall detection algorithm based on single threshold or multi-threshold can achieve relatively ideal detection results. When an athlete falls under a certain state of exercise, due to the interference of behavioral factors, the experimental results of the fall detection algorithm based on a single threshold are not very satisfactory. The fall detection algorithm proposed in the paper optimizes the SMV feature algorithm and introduces energy. The two characteristic values of the inclination angle are used as auxiliary reference objects, so the experimental results are relatively more accurate.

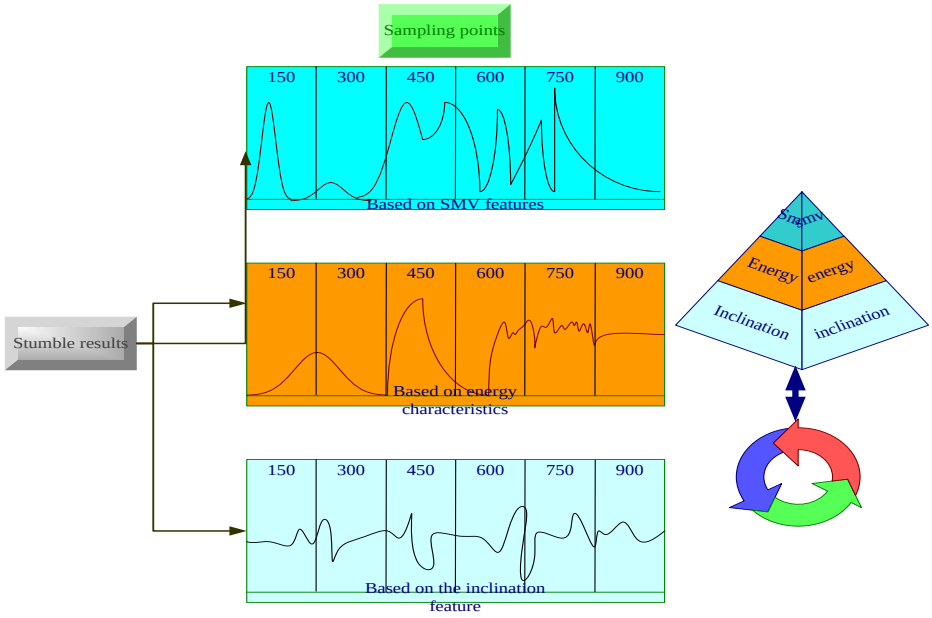

Fig. 7. Fall detection results based on different eigenvalues.

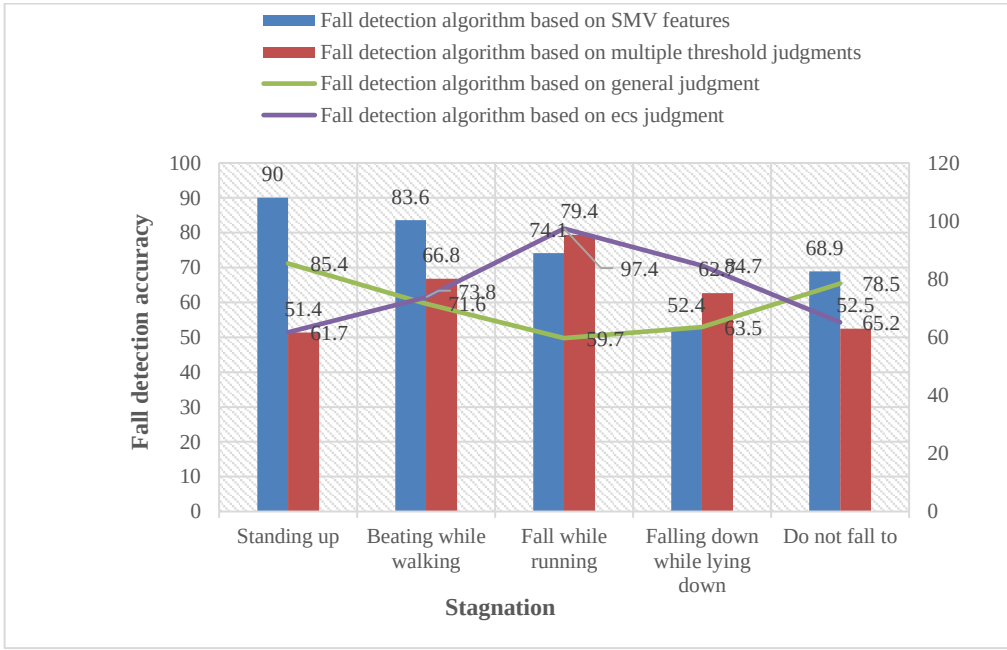

Fig. 8. Fall detection results of the four algorithms in different behavior states.

5.2 Study on the Authenticity of the Monitoring System

The average recognition rate of this monitoring system is 96%. If this requirement can be met, the system is considered to be basically successfully designed. In the previous two chapters, we used graphs to qualitatively illustrate the accuracy of the system's algorithm. In this chapter, we use data to quantitatively illustrate the accuracy of the system's algorithm.

The main selections are cycling and stepping in place for in-depth research, as shown in Table 3.

Table 3. Cycling test results

Experimenter	Actual number of steps	Measurement steps	Step recognition rate
X	55	54	2
	65	61	0.991
Y	55	53	0.97
	65	65	0.99
Average recognition accuracy		0.993	

Table 3 shows the results of the cycling test, which is also an innovative test point of this paper; in this paper, we stipulate that we have stepped on the bicycle for one circle rotation, which means that we have taken a step. It can be seen from the table that the recognition rate of cycling is also very high, almost close to 1, which fully meets the 0.96 recognition requirement of this system. See Table 4 again for the experimental data of stepping in place.

Table 4. Test results of stepping in place

Experimenter	Actual number of steps	Measurement steps	Step recognition rate
A	62	61	1.1
	105	104	0.947
B	59	54	0.93
	99	100	0.95
Average recognition accuracy		0.929	

Table 4 shows the results of the in-situ stepping test. Considering that stepping in place is also an important exercise method, it is also used as the test object. This is also an innovation of this paper. Although, the single recognition rate of standing still did not reach 0.95. However, the total average recognition rate of the nine sports is 0.971, which is already above 0.96; in addition, in terms of proportions, the proportions of the other eight sports are generally larger than those of standing still. Therefore, from the two perspectives of the total average recognition rate and the proportion of sports, it can also be considered that the design requirements of this system have been met.

6. Conclusion

This paper introduces the characteristics and application value of remote sensor monitoring based on machine learning, studies the design and implementation of sensor heart rate monitoring, and designs a simulation system for remote health monitoring. In order to in-depth study the current status of the role of machine learning sensors in wearable heart rate monitoring, this article uses the new and old sensor comparison method, the field survey method and the human sample test method, collects samples, analyzes the machine learning sensor, and streamlines the algorithm. And create a sensor for wearable heart rate monitoring. In the comparative study of the new sensor and the old one, this paper uses the shimmer node on the Tiny-OS platform to collect a total of 36 sets of heart rate data of six people in different exercise states, and uses the new and old algorithms to perform calculations. The results show that the paper proposes the calculation time of the heart rate of the algorithm is 0.21, the traditional ECG algorithm is 0.28, and the new algorithm has lower time complexity. Research on the accuracy of the sensor in the sports test shows that the recognition rate of cycling is almost close to 1.00, which fully meets the 0.96 recognition requirement of this system. Although, the single recognition rate of standing still did not reach 0.95. However, the total average recognition rate of the nine sports is 0.971, which is already above 0.96, which proves that the average recognition rate of the monitoring system is above

96%. The system is considered to be a basic design success. The shortcomings of this paper are: firstly, battery life is a shortcoming of current wearable devices, but the problem has not been solved at present; secondly, the step-counting algorithm and motion process algorithm designed in this paper are very good. Recognize the effect and meet the design requirements of the system; however, the number of experiments is limited after all and cannot provide extensive and strong support. Therefore, in the next stage, I will consider using ultra-low power processors. In addition, rechargeable lithium batteries will be selected as the power supply, and a large number of repetitive and diverse experiments will be verified, so that machine learning sensors can play a greater role in wearable heart rate monitoring.

Author's Contributions

Not applicable.

Funding

None.

Competing Interests

The author declares that he/she has no competing interests.

References

[1] Z. Wang and N. Verma, "A low-energy machine-learning classifier based on clocked comparators for direct inference on analog sensors," *IEEE Transactions on Circuits and Systems I: Regular Papers*, vol. 64, no. 11, pp. 2954-2965, 2017.

[2] W. Zhang, J. Li, Y. Wen, and Y. Luo, "Toward a wearable crowdsource system to monitor respiratory symptoms for pandemic early warning," *IEEE Network*, vol. 35, no. 3, pp. 56-63, 2021.

[3] G. P. Liao, W. Gao, G. J. Yang, and M. F. Guo, "Hydroelectric generating unit fault diagnosis using 1-D convolutional neural network and gated recurrent unit in small hydro," *IEEE Sensors Journal*, vol. 19, no. 20, pp. 9352-9363, 2019.

[4] D. Goyal, S. S. Dhami, and B. S. Pabla, "Non-contact fault diagnosis of bearings in machine learning environment," *IEEE Sensors Journal*, vol. 20, no. 9, pp. 4816-4823, 2020.

[5] W. He, Y. Ye, L. Lu, Y, Cheng, Y. Li, and Z. Wang, "Robust heart rate monitoring for quasi-periodic motions by wrist-type ppg signals," *IEEE Journal of Biomedical and Health Informatics*, vol. 24, no. 3, pp. 636-648, 2020.

[6] Y. Li, B. Dong, E. Chen, X. Wang, and Y. Zhao, "Heart-rate monitoring with an ethyl alpha-cyanoacrylate based fiber Fabry-Perot sensor," *IEEE Journal of Selected Topics in Quantum Electronics*, vol. 27, no. 4, article no. 5600206, 2021. https://doi.org/10.1109/JSTQE.2020.3002084

[7] Q. Xie, Y. Li, G. Wang, and Y. Lian, "An unobtrusive system for heart rate monitoring based on ballistocardiogram using Hilbert transform and Viterbi decoding," *IEEE Journal on Emerging and Selected Topics in Circuits and Systems*, vol. 9, no. 4, pp. 635-644, 2019.

[8] Q. Lin, T. Li, P. M. Shakeel, and R. D. J. Samuel, "Advanced artificial intelligence in heart rate and blood pressure monitoring for stress management," *Journal of Ambient Intelligence and Humanized Computing*, vol. 12, no. 3, pp. 3329-3340, 2021.

[9] G. Cicceri, F. De Vita, D. Bruneo, G. Merlino, and A. Puliafito, "A deep learning approach for pressure ulcer prevention using wearable computing," *Human-centric Computing and Information Sciences*, vol. 10, article no. 5, 2020. https://doi.org/10.1186/s13673-020-0211-8

[10] D. Tang, R. Dai, L. Tang, and X. Li, "Low-rate DoS attack detection based on two-step cluster analysis and UTR analysis," *Human-centric Computing and Information Sciences*, vol. 10, article no. 6, 2020. https://doi.org/10.1186/s13673-020-0210-9

[11] Y. Xin, C. Guo, X. Qi, H. Tian, X. Li, Q. Dai, S. Wang, and C. Wang, "Wearable and unconstrained systems based on PVDF sensors in physiological signals monitoring: a brief review," *Ferroelectrics*, vol. 500, no. 1, pp. 291-300, 2016.

[12] M. A. De Oliveira, A. V. Monteiro, and J. Vieira Filho, "A new structural health monitoring strategy based on PZT sensors and convolutional neural network," *Sensors*, vol. 18, no. 9, article no. 2955, 2018. https://doi.org/10.3390/s18092955

[13] P. Asghari, A. M. Rahmani, and H. Haj Seyyed Javadi, "A medical monitoring scheme and health-medical service composition model in cloud-based IoT platform," *Transactions on Emerging Telecommunications Technologies*, vol. 30, no. 6, article no. e3637, 2019. https://doi.org/10.1002/ett.3637

[14] Z. N. Aghdam, A. M. Rahmani, and M. Hosseinzadeh, "The role of the Internet of Things in healthcare: future trends and challenges," *Computer Methods and Programs in Biomedicine*, vol. 199, article no. 105903, 2021. https://doi.org/10.1016/j.cmpb.2020.105903

[15] F. Ghasemi, A. Rezaee, and A. M. Rahmani, "Structural and behavioral reference model for IoT-based elderly health-care systems in smart home," *International Journal of Communication Systems*, vol. 32, no. 12, article no. e4002, 2019. https://doi.org/10.1002/dac.4002

[16] R. Gonzalez, D. Apostolopoulos, and K. Iagnemma, "Slippage and immobilization detection for planetary exploration rovers via machine learning and proprioceptive sensing," *Journal of Field Robotics*, vol. 35, no. 2, pp. 231-247, 2018.

[17] P. S. Anoop and V. Sugumaran, "Classifying machine learning features extracted from vibration signal with logistic model tree to monitor automobile tyre pressure," *Structural Durability & Health Monitoring*, vol. 11, no. 2, pp. 191-208, 2017.

[18] C. L. Karmen, M. A. Reisfeld, M. K. McIntyre, R. Timmermans, and W. Frishman, "The clinical value of heart rate monitoring using an apple watch," *Cardiology in Review*, vol. 27, no. 2, pp. 60-62, 2019.

[19] Y. Wu, Y. Wang, H. Fang, and F. Wan, "Cooperative learning control of uncertain nonholonomic wheeled mobile robots with state constraints," *Neural Computing and Applications*, vol. 33, no. 24, pp. 17551-17568, 2021.

[20] N. N. Qomariyah, D. Kazakov, and A. N. Fajar, "On the benefit of logic-based machine learning to learn pairwise comparisons," *Bulletin of Electrical Engineering and Informatics*, vol. 9, no. 6, pp. 2637-2649, 2020.

[21] M. Melek, "Diagnosis of COVID-19 and non-COVID-19 patients by classifying only a single cough sound," *Neural Computing and Applications*, vol. 33, no. 24, pp. 17621-17632, 2021.

[22] C. Liu, L. Qi, Q. X. Feng, S. W. Sun, Y. D. Zhang, and X. S. Liu, "Performance of a machine learning-based decision model to help clinicians decide the extent of lymphadenectomy (D1 vs. D2) in gastric cancer before surgical resection," *Abdominal Radiology*, vol. 44, no. 9, pp. 3019-3029, 2019.

[23] H. Kim, E. Ahn, M. Shin, and S. H. Sim, "Crack and noncrack classification from concrete surface images using machine learning," *Structural Health Monitoring*, vol. 18, no. 3, pp. 725-738, 2019.

[24] H. Cho, J. H. Yang, and J. Lee, "A study on the wearable product design for promoting effects of children's exercise: focused on movement-monitoring smart clothing design using textile sensor," *Journal of the Korean Society of Design Culture*, vol. 23, no. 1, pp. 603-612, 2017.

[25] T. D. Ngo, T. D. Tran, M. T. Le, and K. M. Thai, "Machine learning-, rule-and pharmacophore-based classification on the inhibition of P-glycoprotein and NorA," *SAR and QSAR in Environmental Research*, vol. 27, no. 9, pp. 747-780, 2016.